Journal of Sound and Vibration (1997) **200**(3), 261–279

AN ACTIVE MAXIMUM POWER ABSORBER FOR THE REDUCTION OF NOISE AND VIBRATION

N. HIRAMI†

Department of Engineering, University of Cambridge, Trumpington Street, Cambridge CB2 1PZ, England

(*Received* 2 *September* 1994, *and in final form* 27 *June* 1996)

The objective of this work is to assemble and test a non-application-specific active controller for the reduction of noise and vibration and discuss its potential for practical applications. The power absorbed by the controller is taken as a cost function to be maximized. The background theory and essential strategy are reported in the companion paper [1], where it was shown that power absorption maximization within the time taken for a wave emitted by the controller to come back to the control point, i.e., within a single sing-around time, is promising. A maximum power absorber based on this strategy was developed for experimental purposes and the (same) device was applied to three different vibration problems, a string, an acoustic tube and a plate model. These experiments confirmed that the absorber attenuates vibration from a variety of problems effectively, suggesting that the prospects for this controller are encouraging.

1. INTRODUCTION

Active control of noise and vibration aims to supplement a wave field with destructively interfering secondary waves to reduce the sum as much as possible. This technique has been researched extensively and seems to have become an alternative approach for the reduction of noise and vibration (see the review by Ffowcs Williams [2]). Although this technique is well established, the author pointed out that these applications tend to be application specific and proposed a new control strategy which is non-application-specific [1]. In the strategy, power absorbed by the controller is taken as a cost function to be maximized and the optimization process was carried out within the time taken for a wave emitted by the controller to come back to the control point: i.e., within a sing-around time. A new control strategy based on the velocity feedback was then proposed. The purpose of this paper is to demonstrate this idea experimentally and discuss its potential for practical applications. The idea of maximum power absorption was investigated experimentally by Redman-White *et al*. [3] and Guicking *et al*. [4]; however, their work is restricted to an infinite system, in which only travelling waves are considered as a control target. In these infinite cases there is no danger of increase in power input from the primary source due to the maximization of the power absorbed, which may increase the energy in the system. On the other hand, the focus here will be on the control of nearly resonant systems, which is relatively untouched and one of the important aspects of vibration problems.

† Present address: Mazda Motor Corporation, 3-1, Shinchi, Fuchu-cho, Aki-gun, Hiroshima 733, Japan.

0022–460X/97/080261 + 19 $25.00/0/sv960661

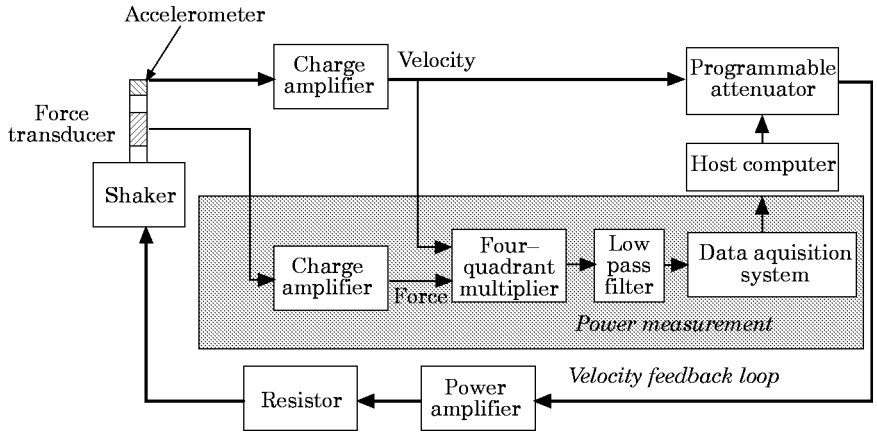

Figure 1. The experimental configuration of the maximum power absorber.

2. DEVELOPMENT OF THE MAXIMUM POWER ABSORBER

2.1. SYSTEM CONFIGURATION

The schematic configuration of the proposed maximum power absorber is shown in Figure 1. The system undertakes two tasks at the same time. One is the measurement of the power absorbed by the shaker, and the other is to feed back the velocity to the shaker with a certain gain. The gain is attenuated by the host computer based on the measured power. The installation of the force transducer and accelerometers onto the shaker is shown in Figure 2. The force transducer (Kistler 9301A) is attached with screws to the table of the shaker and the clamping device. The clamp supports two accelerometers as shown in the figure. The clamping device was specially designed with a triangular section so that only a translational force is applied to the control object, a string type object being assumed. Note that a two-pole Bessel low-pass filter with a cut-off frequency of 300 Hz was used as an anti-aliasing filter. This filter features maximally flat time delay within its passband. Since it is wished to control signals from a single frequency to broadband frequency vibration, the filter is required to pass a wide range of frequencies with a constant time delay. For this reason, the Bessel filter was chosen. A simple resistor was put in the feedback circuit to reduce an initial electrical damping by back EMF.

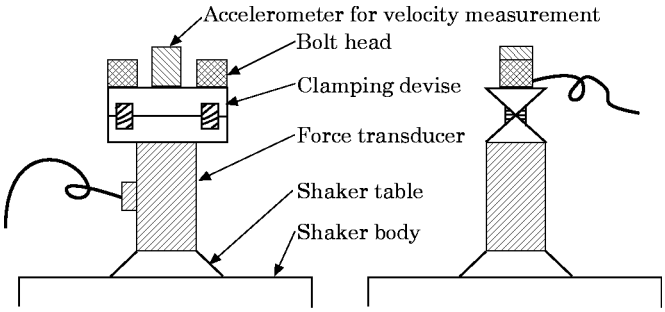

Figure 2. The installation of the force transducer and accelerometers. (a) Front view; (b) side view.

2.2. ELECTROMECHANICAL SYSTEM

The electromechanical system in the closed loop is shown in Figure 3. The electrical part of the model consists of a simple *RL* circuit, while the mechanical part of the shaker is modelled by a one-degree-of-freedom system as shown in Figure 4. The electrical system and the mechanical system introduced above are coupled at the position of the coil assembly in the shaker. The power amplifier amplifies the measured velocity signal to produce a voltage in the *RL* circuit, providing the current to drive the coil assembly. When a current I in a conductor of length l is placed perpendicular to the magnetic field B, a force BIl at right angles to the plane of I is experienced by the conductor. At the same time, when a conductor of length l moves at a velocity v through a constant magnetic field B at right angles to the direction of the field, a voltage Bvl arises between the ends of the conductor. In our case, the coil assembly corresponds to the conductor. Considering these

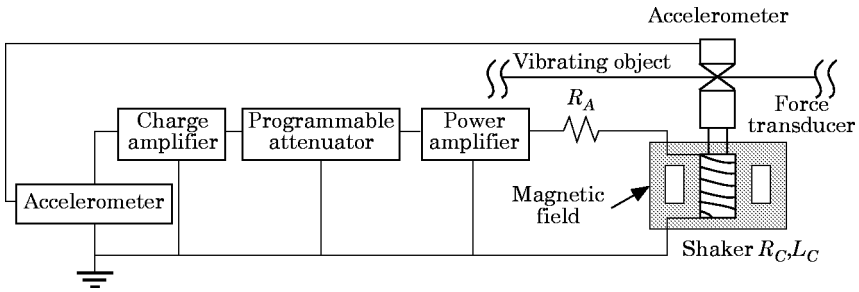

Figure 3. The feedback circuit.

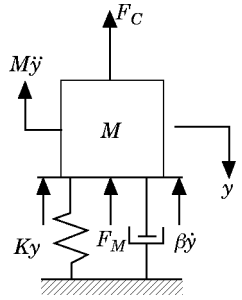

Figure 4. The mechanical vibration model for the shaker. F_c, force applied from the control object; F_M, force applied from the magnetic field.

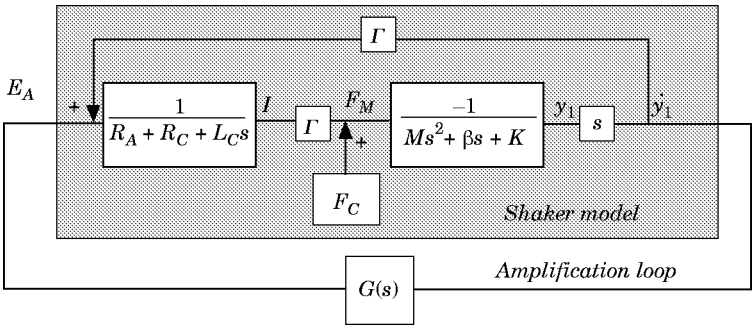

Figure 5. The block diagram for the control system.

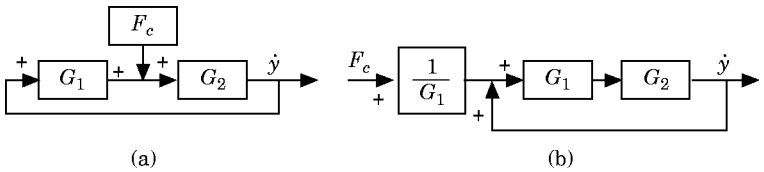

Figure 6. The block diagram of the feedback loop with disturbance. (a) F_c as a disturbance; (b) F_c as an input.

conditions and the equilibrium of the forces, one obtains the block diagram for the closed loop system shown in Figure 5. In the figure, an amplification loop from the accelerometer to the power amplifier is symbolized by $G(s)$, where s is a complex frequency variable, and $\Gamma = Bl$. The feedback gain from the velocity to the force applied to the control object by the shaker is

$$Z = \frac{G(s)+\Gamma}{R_A + R_C + L_C s}\Gamma + Ms + \beta + \frac{K}{s}. \tag{1}$$

2.3. STABILITY STUDY

Consider again the feedback system shown in Figure 5. An external force F_C is applied to the closed loop system. This force can be regarded as a "disturbance"; the system is depicted in Figure 6(a). The output velocity is

$$\dot{y} = \frac{G_1 G_2}{1 - G_1 G_2}\frac{1}{G_1}F_C, \tag{2}$$

which indicates that the system can be alternatively regarded as in Figure 6(b). The stability condition of the feedback system can be obtained by examining the closed loop comprised of G_1 and G_2 in series, which is exactly the same as the closed loop system in Figure 5.

The overall open loop transfer function is given in Figure 7, predictions being compared with measurements. The results support the validity of the predicted transfer functions. The stability criterion for simple negative feedback control suggests that if a gain with zero phase shift exceeds 0 dB, the signal amplitude increases at every iteration of the feedback when the loop is closed, leading to instability. From Figure 7, one sees that the gain margin

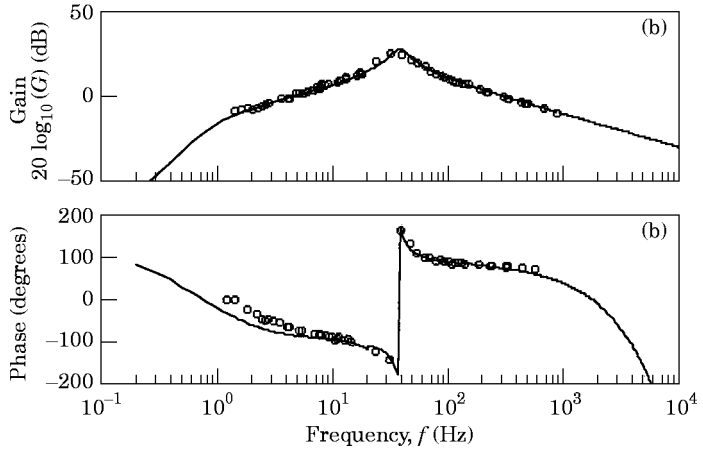

Figure 7. The bode plot for the open loop transfer function; amplified maximally (40 dB). —, predicted; ○○○, measured.

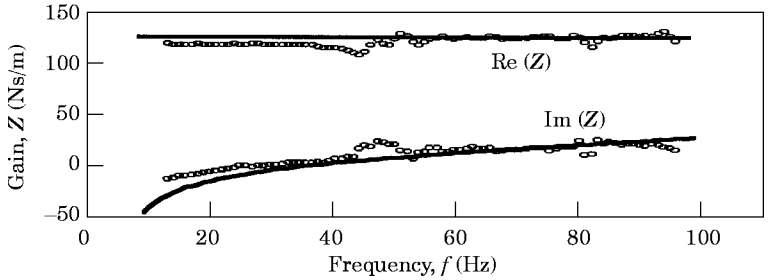

Figure 8. The transfer function between velocity and force; amplification loop gain $G_A = 1060$ V s/m. —, predicted; ○○○, measured, Z = force/velocity.

is 14 dB (at 1·8 kHz) and the phase margin is 50–70 degrees (at 3·5 Hz). These margins guarantee the stability of the feedback system.

2.4. FEEDBACK GAIN

The feedback gain from the velocity of the control point to the force applied to the control object is given by equation (1). The frequency response of the gain is obtained by putting $s = \mathrm{i}\omega$ into that equation: i.e.,

$$Z(\mathrm{i}\omega) = \frac{G(\mathrm{i}\omega)+\Gamma}{R_A + R_C + L_C\omega\mathrm{i}}\,\Gamma + M\omega\mathrm{i} + \beta - \frac{K}{\omega}\,\mathrm{i}. \tag{3}$$

Consider the frequency band between 5 Hz and 300 Hz. Within this frequency band $G(\mathrm{i}\omega)$ has a flat response. Therefore, it is reasonable to put $G(\mathrm{i}\omega) = G_A$ into equation (3). By doing so and taking the real and imaginary parts, one obtains

$$Z_r = \frac{(G_A + \Gamma)(R_A + R_C)}{(R_A + R_C)^2 + L_C^2\omega^2}\,\Gamma + \beta, \qquad Z_i = \frac{-(G_A + \Gamma)L_C\omega}{(R_A + R_C)^2 + L_C^2\omega^2}\,\Gamma + M\omega - \frac{K}{\omega}. \tag{4, 5}$$

A comparison of the measured gains with predicted ones is shown in Figure 8. The comparison shows good agreement, supporting the validity of equations (4) and (5). To examine the linearity of the real part of the feedback gain against the amplification-loop gain, a relationship between the two gains was obtained. Shown in Figure 9 is the measured and predicted relationship, which clearly indicates the linearity of the two. This means that one can increase the real part of the feedback gain by simply increasing the amplification-loop gain.

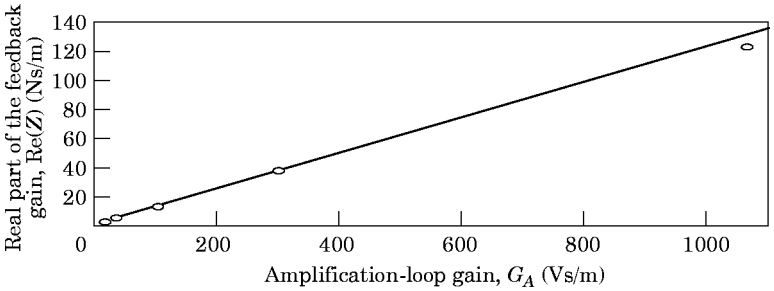

Figure 9. The linear relationship between feedback voltage gain and feedback gain. $G_A = E_A/\dot{y}$, measured when $\omega = 344$ rad/s, ○○○, measured; —, predicted.

2.5. POWER MEASUREMENT AND OPTIMAL GAIN SEARCH

Described here is an algorithm to calculate power absorbed and to find an optimal feedback gain based on the measurement. The basic idea is the same as that reported earlier [1]. However, since it is difficult to predict the sing-around time, and even if it is predicted the time is expected to be very short, further refinements were made to realize the gain search.

A routine for deciding the sampling period was introduced. Power is measured for a certain period, followed by a FFT analysis of the data to find dominant frequencies. If a single frequency is dominant, double the period of the frequency is chosen as the basic sampling period. If a few frequencies are dominant, the largest beat period is calculated, and the double period used as the basic sampling period. When the sing-around time is not known, the fundamental sampling period is used, which means that one complete cycle of the wave is sampled. On the other hand, when the sing-around time is known, a multiple of the basic period which does not exceed the sing-around time is selected. If many frequencies are prominent, the wave is regarded as a broadband noise, and a prescribed value is set for the sampling period.

In a theoretical work [1], a method of feedback gain optimization was introduced, a method based upon the assumption that the sing-around time is long enough for multiple gain changes to occur; the gain change and data sampling are undertaken simultaneously. However, in a real system, one does not necessarily know the sing-around time and an inevitable time delay exists. In order to solve this problem, a pair-comparison method is proposed. This method is illustrated in Figure 10. After keeping a Gain 1 for a while, the controller samples power. Then it changes the gain to Gain 2 and samples power again, followed by next gain prediction. If the power is increasing, i.e., Power(Gain 2) > Power(Gain 1), the controller keeps Gain 2, and repeats the procedure. However, if the power is decreasing, i.e., Power(Gain 2) < Power(Gain 1), the controller sets a new Gain 1 and repeats the gain search continuously: i.e., the system is adaptive.

The next gain prediction is based upon the modified Davies, Swann and Campey method [5]. This method is basically a gradient method, enabling the above pair-comparison to be made. After the measured power decreases for any reason for the first time, the controller is programmed to use the following method to keep adapting the control object. If the power is increasing, the previous gain (Gain 2) is retained, and the next value made is 120% of this gain. On the other hand, if the power is decreasing, the gain set to 90% of the previous Gain 1 level, and the next to 120% of that. These percentages can be altered.

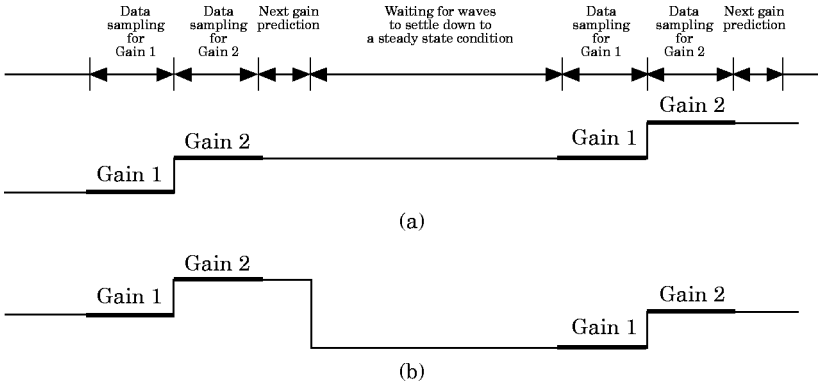

Figure 10. A pair comparison method. (a) Power(Gain 2) > Power(Gain 1); (b) Power(Gain 2) < Power(Gain 1).

When the power measured is low in amplitude, e.g., in a case in which the control point is near to a node of a resonance mode, inevitable errors in measurement make it difficult to assess the differences between the two powers. When broadband random noise is controlled, the sampled data should be statistically stationary. An increased rate of sampling is expected to be beneficial for both these problems. Therefore, a repetition of the gain search with the same Gain 1 and Gain 2 was introduced. This procedure is exactly the same as the one described in Figure 10, except that it keeps the same gains.

It is evident that the time-averaged power excludes the effect of the imaginary part of the feedback gain Z; therefore, the force measured at the transducer position and measured velocity are multiplied to give a power upon which a control gain is optimized.

3. THE STRING MODEL INVESTIGATION

3.1. STRING MODEL

An experimental string model was constructed to be controlled by the developed maximum power absorber. The configuration of the string model is shown in Figure 11. A piano bass string (copper wound string; 2330 mm, 388·7 g) was selected. The left end of the string was supported firmly with a steel block. To reduce the effect of reflected waves from the rigid support on the primary shaker, the extended wire was damped with a felt absorber. The right end was rigidly supported by a similar device. A shaker with a mass of 606 g and a commercially available auxiliary suspension were used as a primary shaker to generate vibration with constant displacement. The system parameters of the string system were as follows: density of the string, $\rho = 0{\cdot}167$ kg/m; tension of the string, $T = 377$ N; speed of the waves, $c = 47{\cdot}5$ m/s.

3.2. EFFECTIVENESS OF THE CONTROL

The string model was excited at its third, fifth and seventh resonant modes, the anti-nodes of which coincide with the control point, and controlled by the maximum power absorber. The modes are the modes of the string between the primary shaker and the right-hand rigid support, and because of the installation of the secondary shaker, the frequencies are slightly different from those of a simple string. In Figure 12 is shown the vibration level (peak-to-peak value) at the control point, which is used as an indicator of control effectiveness. For example, in Figure 12(b), we see that the initial vibration level is reduced by 15 dB after placement of the shaker (due to the mode change as well as damping effect), and another 10 dB reduction is achieved by active control (repetition number of the sampling was one in this measurement). The remaining results show similar reductions, showing the effectiveness of this control strategy. The corresponding

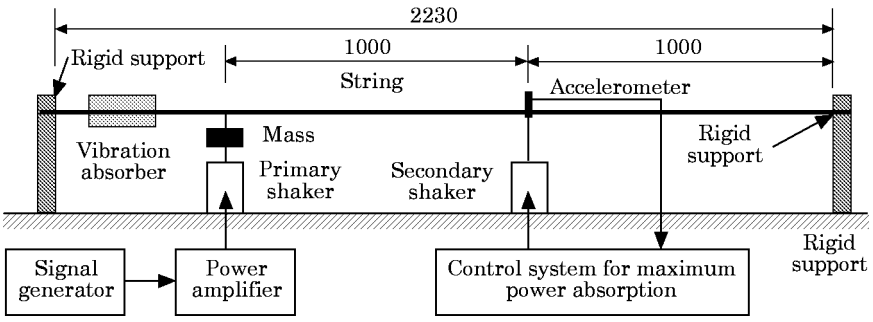

Figure 11. The experimental string model. Lengths in mm.

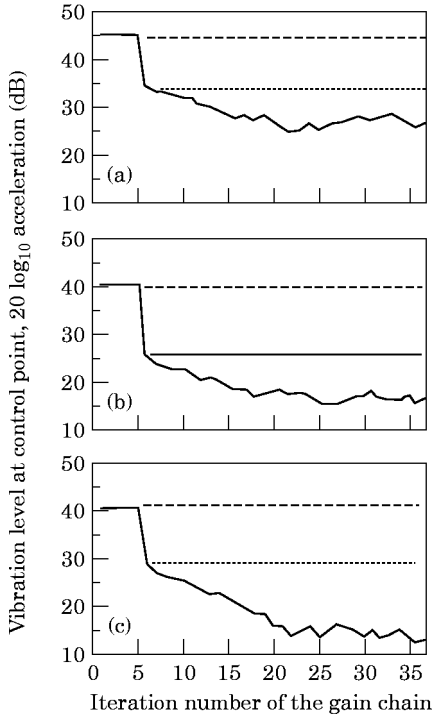

Figure 12. The effectiveness of the active control. (a) Third mode ($f = 35$ Hz); (b) fifth mode ($f = 55$ Hz); (c) seventh mode ($f = 78$ Hz). – – –, initial vibration level; ·····, after placing the shaker; —, after active control.

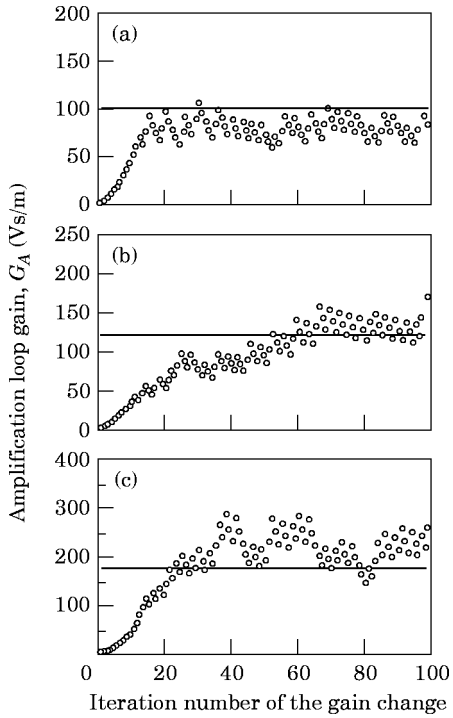

Figure 13. The convergence of the measured amplification loop gain. (a) Third mode ($f = 35$ Hz); (b) fifth mode ($f = 55$ Hz); (c) seventh mode ($f = 78$ Hz). —, predicted optimal gain; ○○○, measured.

convergence of the amplification-loop gain is shown in Figure 13. While the third and fifth modes show good convergence to the predicted optimal gain, the seventh mode shows a slight fluctuation.

It has been seen [1] that the optimal gain is given by a feedback gain, Z, which maximizes

$$k_{pr} = \frac{Z_r}{\{(2T/c) + Z_r\}^2 + Z_i^2}, \tag{6}$$

where Z_r and Z_i are the real and imaginary parts of Z, and the number is found to be twice the characteristic impedance of the string, which is a pure real number. In this experiment, the impedance is

$$T/c = 7{\cdot}94 \text{ N s/m}, \tag{7}$$

so the optimal gain is

$$Z_{opt} = 15{\cdot}9 \text{ N s/m}. \tag{8}$$

However, the control system is identified to have a gain given by equations (4) and (5) with G_A as a single variable parameter. Therefore, one has to substitute equations (4) and (5) into equation (6) and then find the value of G_A which maximizes the equation. In other words, power is maximized with the limitation of the feedback loop's characteristics. To illustrate this process, equation (6) for this model is plotted in Figure 14. It is clear that the maximum power is absorbed by the purely real feedback gain given by equation (8), and if there is a constraint between the real and imaginary parts of Z, the maximum gain search is undertaken along its trajectory on the power coefficient curve. The trajectory of the three previous different frequencies against the amplification-loop gain is shown in Figure 15. This figure indicates that the optimum gain increases according to the frequency, and also that the peak of the trajectory becomes dull. This tendency makes it difficult for the controller to find the optimal gain. This characteristic explains the fluctuation seen in Figure 13(c).

Although the optimal gain search becomes difficult as the frequency increases, the idea of maximum power absorption works as a fundamental principle. This difficulty can be overcome by the following measures: (1) increase the accuracy of the power measurement —this should be possible by increasing the iteration number of the power measurement, as explained above; (2) change the natural frequency of the shaker system so that the frequency is closer to the frequency of the control object—for instance, by providing

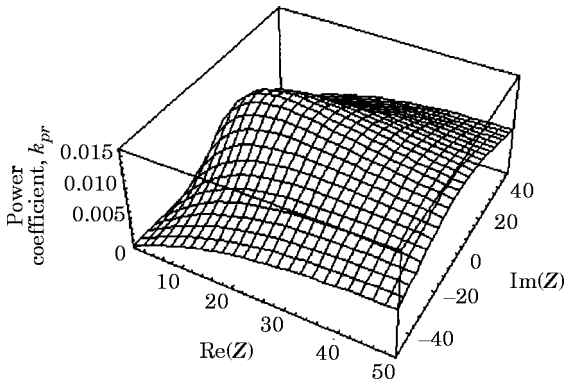

Figure 14. The effectiveness of the feedback gain on the power coefficient.

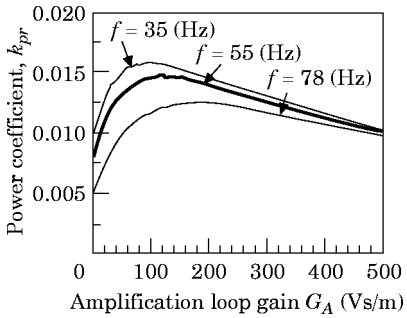

Figure 15. The power coefficient for different frequencies.

an auxiliary suspension or by replacing the shaker; (3) put an electrical compensator in the feedback path so that the level of the imaginary part of the feedback gain decreases.

3.3. BROADBAND RANDOM VIBRATION CONTROL

The maximum power absorber was applied to the problem of suppressing broadband vibration excitation which is assumed to be statistically stationary. The string was driven by the primary shaker with white noise (cut-off frequency 150 Hz), which excited a wide range of frequencies. In order for the controller to assess significant changes in the power absorbed due to gain changes, the sampling period is required to be reasonably long. Since the sampling of the power is undertaken within a short specified time cycle, the repetition of this sampling must be increased. The effectiveness of increasing the iteration number is shown in Figure 16. Plotted in the figure are the amplification loop gain history with the optimal gain for 200 Hz, and the lowest optimal gain as a reference. It is indicated in this figure that the increase in the iteration number stabilizes the convergence of the gain search.

As has been reported [1], the effectiveness of the active control depends on the location of the control point relative to the vibration modes of the control object. If the controller were placed in the middle of the string, the controller would suppress half the modes; however, if it were slightly offset from the middle, it would control most of the modes. Based on this theoretical study, the controller was placed at two positions, the middle of the string and 50 mm offset from the middle. The result of the control is shown in Figure 17. The acceleration level, at a distance of 450 mm from the right end, is plotted in the figure. Parts (a) and (b) show the power spectral density of the acceleration at both the middle of the string and with an offset. Although both show a considerable reduction in the acceleration level (in this case due to initially inherent damping inside the

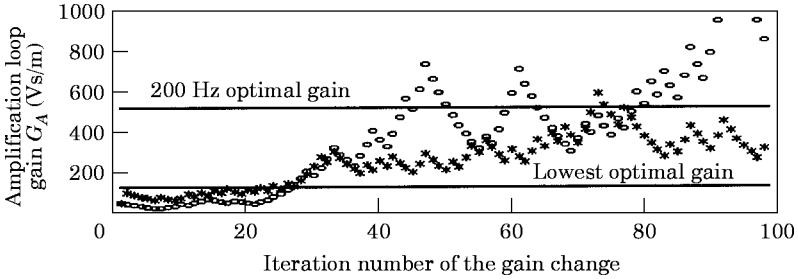

Figure 16. The convergence of the measured amplification loop gain for broadband noise excitation. Iteration numbers: ○○○, 1; ***, 20.

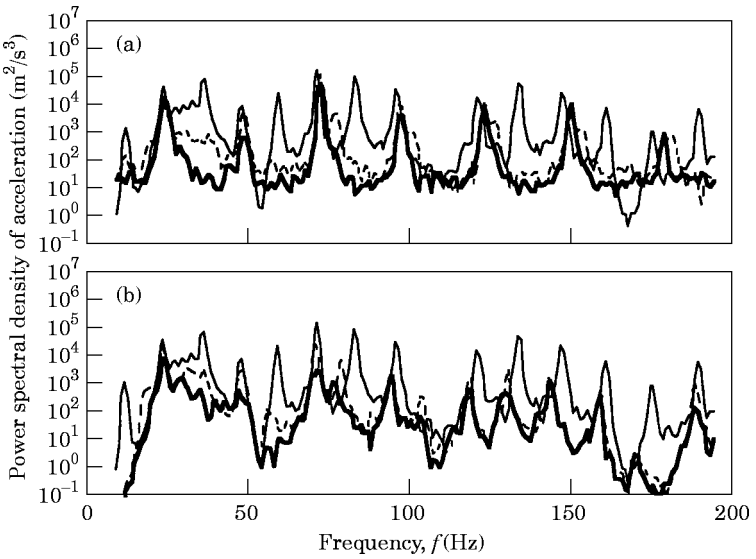

Figure 17. The acceleration at $x = 450$ mm from the right end; excited with white noise (cut-off frequency 150 Hz). (a) Controlled at $x = 1000$ mm from the right end (at the middle of the string); (b) controlled at $x = 950$ mm from the right end. —, no control; – – –, after placing shaker; **—**, active control.

shaker; placing the shaker appears to suppress vibration considerably), the former suppresses only half of the vibration modes. On the other hand, the latter suppresses almost all of the modes. These results indicate the effectiveness of the maximum power absorber for broadband vibration, and also the effectiveness of controlling the object by locating the shaker with an offset from the middle point of the system.

3.4. COMPARISON OF POWER ABSORPTION CRITERIA

3.4.1. *Maximum power absorption*

The idea of maximum power absorption was categorized into two different control strategies [1]. One was to absorb, but not to change, the incoming power as much as possible, and the other maximizes the power absorbed in the steady state, where the incoming power may be affected by the controller. The maximum power absorber was designed to realize the former strategy. However, the latter can also be realized with a slight modification to the control system. Since the strategy aims to increase the power absorbed in the steady state, an increase in the sampling duration of power absorbed beyond a sing-around time should enable the control strategy. This idea is supported in Figure 18. Shown in the figure is the power absorbed by Gain 2 divided by the power absorbed by Gain 1 (Gain 1 = 23·76 and Gain 2 = 47·52 V s/m) against sampling duration for the frequency 35 Hz; under this condition Gain 2 absorbs more power than Gain 1 (this is indicated in Figure 13(a)): i.e., the ratio must be larger than 1. This result indicates the following two points: (1) the averaged power absorbed within a sing-around time gives information about whether or not the gain change will make the controller absorb all the incoming power; and (2) an increase in the sampling duration gradually makes the controller absorb power at the steady state condition. Given these results, the controller was operated with a much longer sampling period than the sing-around time. The behaviour of the controller is shown in Figure 19(a). The string was initially under control with a high amplification loop gain of 530 V s/m; the vibration level was low at this

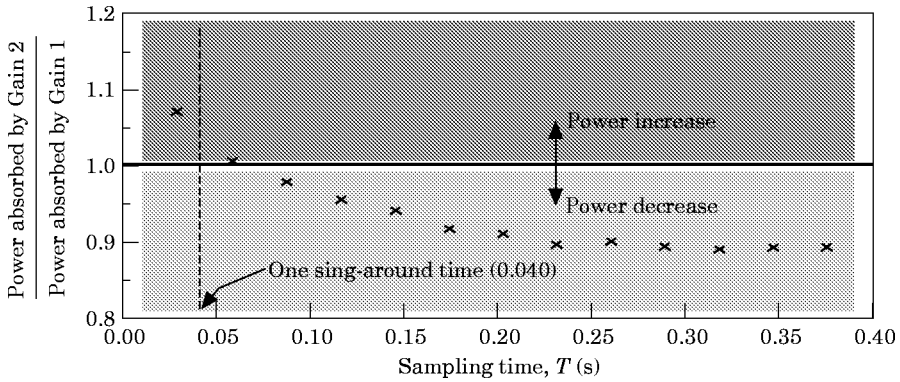

Figure 18. The effectiveness of the sampling time on the power measurement. Gain 1 (=23·76 V s/m) and Gain 2 (=47·52 V s/m) are the two successive gain settings in the gain iteration scheme described in section 2.5.

condition. As expected, the controller changes the feedback gain less and less as the measured power absorbed becomes larger and larger, leading to a higher energy level in the string. Figure 19(b), which shows the vibration level at the control point, supports this tendency. These studies have made the difference between the two control strategies clear, and reaffirmed the importance of the sampling period being less than one sing-around time.

3.4.2. *Maximum increase of the feedback gain*

The results shown in Figures 12 and 13 suggest that vibration tends to be suppressed effectively as the value of the optimal feedback gain increases. This effect is due to a widely known velocity feedback control, and the effectiveness of increasing the gain is also well known. For example, Rockwell and Lawther [6] increased the feedback gain as much as possible while maintaining stability. It is obvious that this increase leads to zero power absorption, since there will be no energy to be absorbed when the control point is stationary. Therefore, from the viewpoint of power absorption, this infinite increase may be regarded as a "zero power absorption strategy". This control can be achieved with the present control system by changing the objective function from power absorbed to the

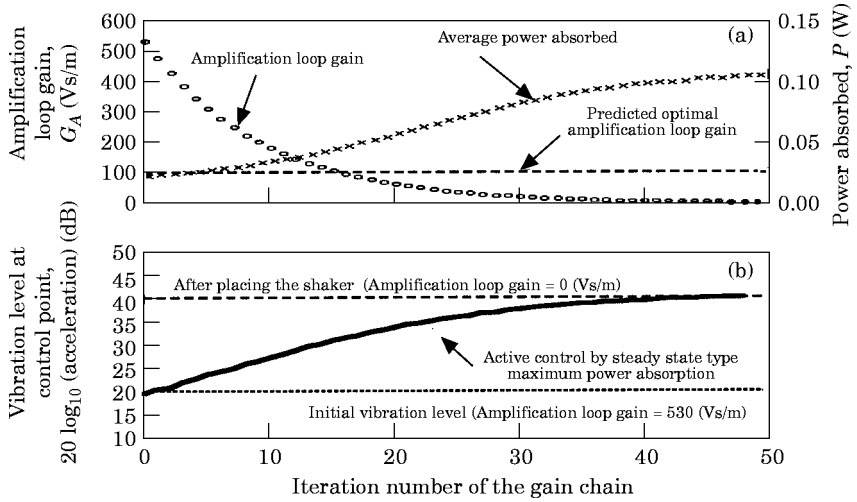

Figure 19. The defectiveness of steady state type maximum power absorption; sampling time = 13 × period of the wave (f = 35 Hz). (a) Convergence of the amplification loop gain; (b) vibration level at control point.

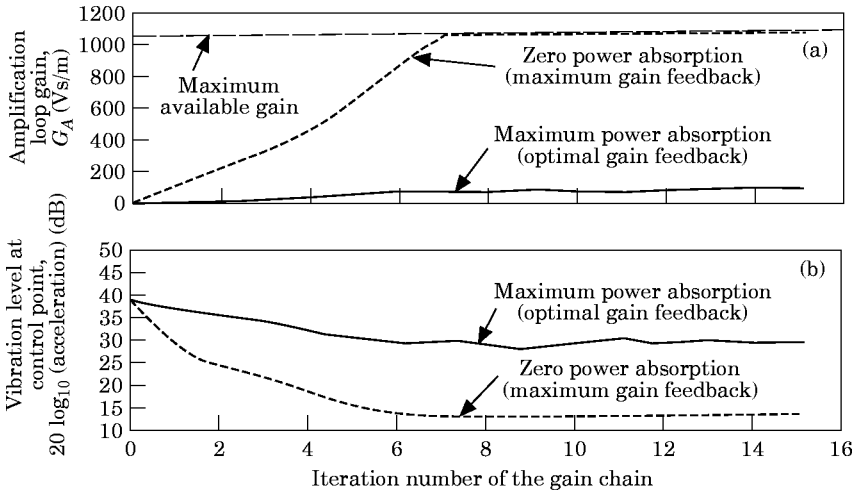

Figure 20. The effectiveness of maximum gain feedback; excited at a frequency of 35 Hz. (a) Amplification loop gain; (b) vibration level at control position.

inverse of the power absorbed. The maximum power absorber was modified according to this idea. Its measured effectiveness, compared with the effectiveness of maximum power absorption, is shown in Figure 20. As expected, this control strategy suppresses the vibration better.

This infinite increase of the feedback gain is physically constraining the point of control, which means that the control is changing the dynamic characteristics of the structure, creating other vibration modes. To demonstrate this, the secondary shaker was placed at 700 mm from the right end, and the acceleration at 1350 mm from the right end was measured. The string was driven by the primary shaker at a frequency of 18 Hz, which corresponds to the first mode of the string between the primary and secondary shakers. As shown in Figure 21(a), the amplification-loop gain for the zero power absorption increases steadily up to the maximum gain available in the control system. As the gain

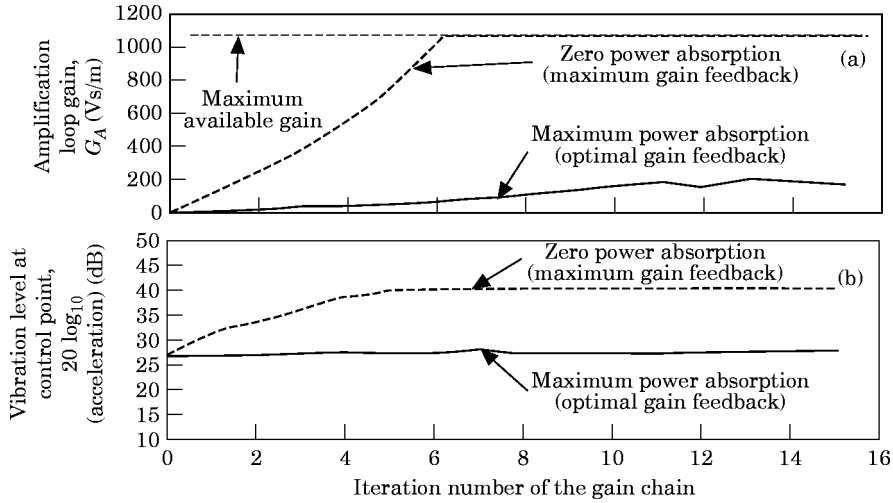

Figure 21. The defectiveness of maximum gain feedback; excited at a frequency of 18 Hz. (a) Amplification loop gain; (b) vibration level at control position.

increases, the vibration level also increases, whereas the optimal gain feedback keeps the level low, as shown in Figure 21(b).

These studies suggest that although an infinite increase in the feedback gain is effective in suppressing the vibration, there is a possibility that unexpected resonance modes may occur, which makes the system susceptible at other frequencies. Furthermore, the instability study described in the previous section indicates that a large increase in the feedback gain inevitably leads to potential instability. In this respect, this feedback control system is required to assess the dynamic characteristics of the control object before the application of maximum feedback control to identify the limitation, which makes the control more complicated.

Therefore, one can state that the use of maximum feedback gain is an application-specific strategy. It should be noted that, if the problem is not specific, the maximum power absorption is superior to this strategy.

4. CONTROL OF THE TUBE MODEL

Described here is an application of the maximum power absorber to an enclosed sound field to demonstrate its versatility. Sound in a simple metal tube is attenuated by the same system placed at the end of the tube.

4.1. TUBE MODEL

A simple steel pipe (6000 mm in length and 80 mm in inner diameter) was selected. The schematic illustration of the model is shown in Figure 22. The primary speaker is placed at the left flange of the tube. The microphone is placed at a distance of 1600 mm from the left end inside the tube to monitor the sound pressure level. The control device, consisting of an accelerometer, a force transducer and a shaker, is connected to a diaphragm (diameter 100 mm) furnished in the sound control box with special arrangements for attachment (see Figure 23). To keep the section area constant, the

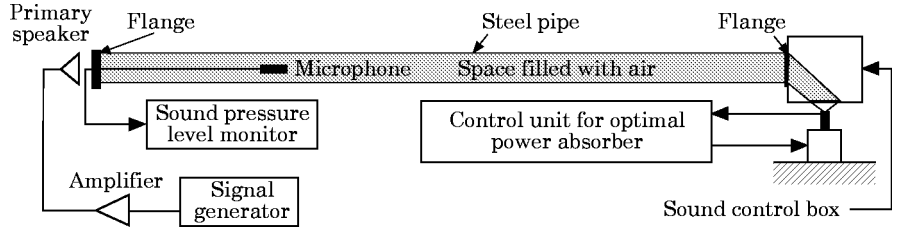

Figure 22. The schematic configuration of the experimental system.

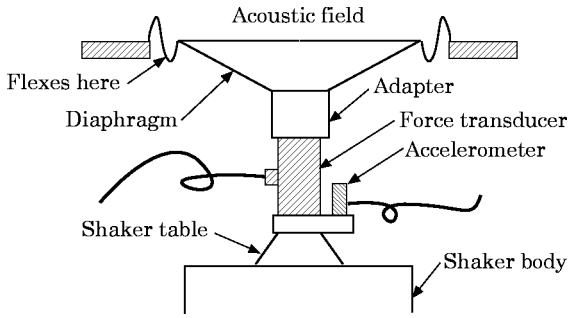

Figure 23. The maximum power absorber applied for sound control.

volume inside the box is reduced with Plasticine, varnished on the surface. The control system is exactly the same as the one applied to the experimental string model in the last section save for the special attachment.

4.2. THE EFFECTIVENESS OF THE CONTROL

4.2.1. *Single frequency excitation*

An acoustic sound field in the tube was excited by the primary speaker with its second, third, fourth, fifth and sixth resonance frequencies (41, 69, 97, 124 and 151 Hz, respectively). The history of the amplification-loop gain alteration, and pressure level was recorded for each resonance frequency. The data sampling period was made a multiple of the fundamental period and was not allowed to exceed one sing-around time (0·035 s), and the iteration number was 5. It was seen that the control system has a limitation for an effective frequency band due to phase shift in the feedback loop. This phase shift occurs mostly in the shaker, which is a single mass and spring system. Feedback of acceleration effectively changes the mass artificially. This thought was adapted for the control system and acceleration with a fixed gain was fed back as well as velocity. The amplification-loop gain and pressure level reduction achieved are shown in Figures 24(a) and (b). For all frequencies, the amplification loop gain tends to converge to a certain value as the number of iterations increases, and the sound pressure level reduction also converges to a certain value. The different attenuations achieved at different frequencies are due to the inevitable phase shift in the feedback loop, which increases the optimal power absorbing point and reduces the power absorbing ability. This is inferred from Figure 15. This result, however, indicates that the optimal power absorber, which has been shown to work on the string, is also directly applicable to an enclosed sound field without any change to either the system hardware or software; our control strategy is evidently versatile.

4.2.2. *Broadband random excitation*

The sound field is excited by the primary speaker with broadband noise (0.2–150 Hz). An optimal gain search was carried out by the control system (iteration number 20). In

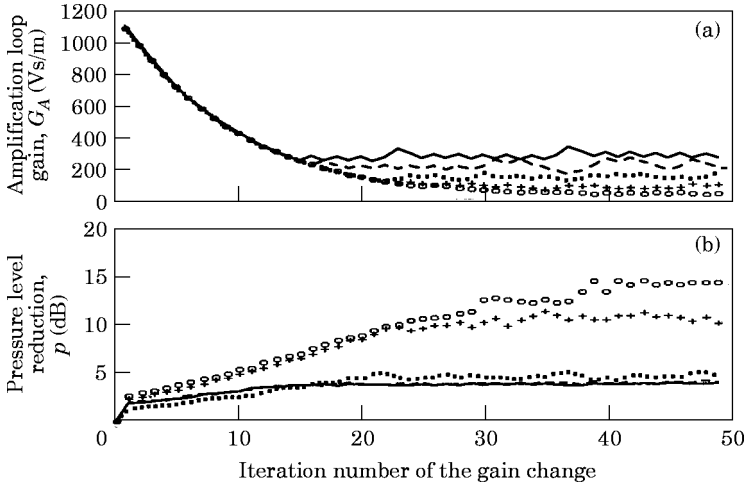

Figure 24. The effectiveness of active control on the tube model; single frequency excitation with acceleration feedback. (a) The convergence of the measured amplification loop gain; (b) pressure level reduction at $x = 1600$ mm. f (Hz); ○○○, 41; + + +, 69; • • • •, 97; – – –, 124; —, 151.

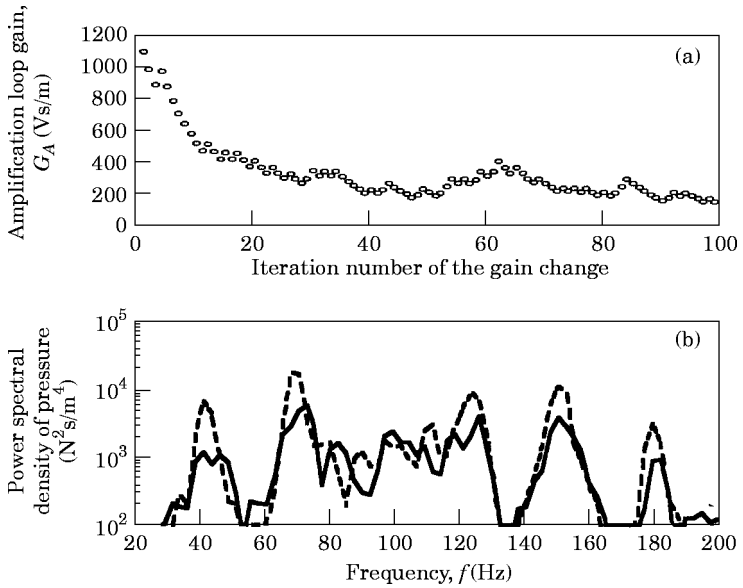

Figure 25. The effectiveness of active control on the tube model; broadband random excitation (0.2–150 Hz). (a) The convergence of the measured amplification loop gain. (b) Pressure at $x = 1600$ mm from the left end: – – –, no control; —, active control.

Figure 25(a) is shown the gain history, indicating that the gain converges within a band between 200 and 400 V s/m, although it fluctuates in the band. This phenomenon is explained as follows. If there were no phase shift in the feedback loop, the gain would converge to an optimal value. However, since phase shift does occur, the optimal point of the power coefficient varies depending on the frequency. These various optimal points make it impossible for the controller to converge to one value. Thereby the gain fluctuates in a certain frequency band which is determined by the influential modes of the system at that instant.

The effectiveness of the optimal control on the power spectral density of sound pressure in the tube is shown in Figure 25(b). Typical measured pressures are shown in the figure. This result shows that the sound pressure is attenuated over a wide range of frequencies by the active control though a slight increase in sound pressure is seen due to varied randomness of the sound pressure at each measurement, indicating that our optimal power absorber is applicable to an enclosed broadband sound field.

5. CONTROL OF THE PLATE MODEL

The maximum power absorber developed has been applied to two one-dimensional wave fields, showing its effectiveness on both. The ultimate objective is to control unidentified vibrating objects, where the waves are not nearly so simple, so application of the control system to two-dimensional waves in a panel has also been made.

5.1. PLATE MODEL

A thin steel rectangular plate ($2000 \times 1000 \times 1{\cdot}2$ mm) was selected. A schematic illustration is shown in Figure 26. The plate is suspended at the centres of each of the four sides by piano wire. The primary shaker is placed at one corner of the plate, and the

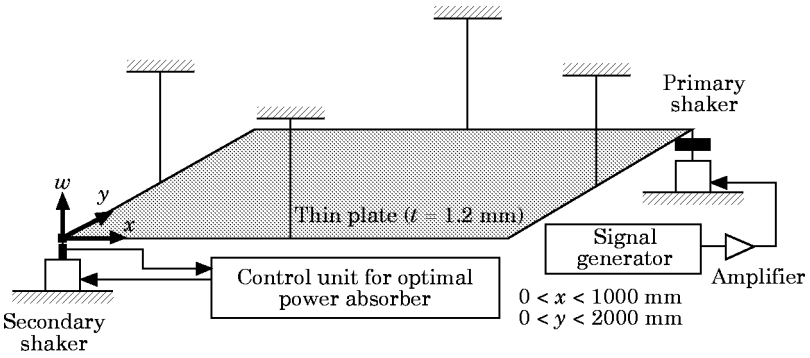

Figure 26. The schematic configuration of the experimental plate model.

secondary shaker at the diagonally opposite corner. The control system is exactly the same as previously used and described.

5.2. THE EFFECTIVENESS OF CONTROL

The convergence of the amplification loop gain for one of the resonance frequencies of the plate (64 Hz) is shown in Figure 27(a). Three sampling periods were selected. The first one was within one sing-around time which is 0·17 s (sampling period $T_{SP} = 0{\cdot}016$ s).

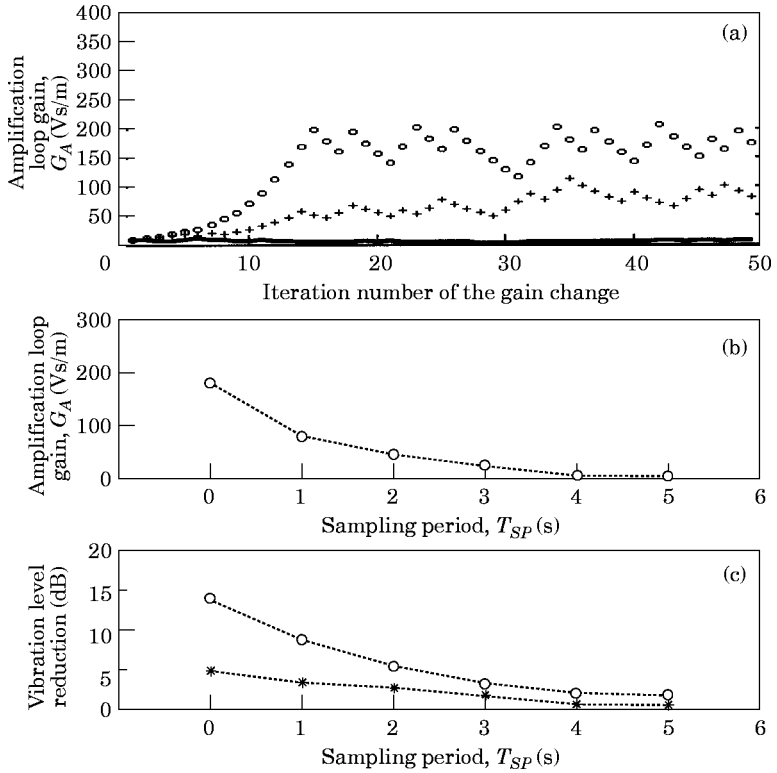

Figure 27. The effect of sampling time. (a) The convergence of the measured amplification loop gain; (b) amplification loop gain at steady state condition; (c) vibration level reduction. Key for (a): ○○○, optimal control ($T_{SP} = 0{\cdot}016$ s); + + +, steady state control ($T_{SP} = 1$ s); —, steady state control ($T_{SP} = 5$ s). Key for (c): ○, point A, (0, 0)-control point; ∗, point B, (800, 200).

The other two, $T_{SP} = 1{\cdot}0$ s and $T_{SP} = 5{\cdot}0$ s, were selected to exceed one sing-around time. It is shown in the figure that the gain converges to a certain value for all sampling periods. However, it is seen that the gain converges to a smaller value as the sampling period increases. This tendency is depicted in Figure 27(b), and the corresponding vibration reduction at point A (the control point) and at point B ($x = 800$ mm, $y = 200$ mm) is shown in Figure 27(c). These figures clearly indicate that as the sampling period increases the amplification loop gain decreases, and the vibration reduction also decreases.

When studying the string model, it was found that if the sampling period exceeds one sing-around time, the controller tends to lead the gain to a smaller value, and becomes less effective. This tendency was explained as follows. When the sampling time is more than one sing-around time, the controller influences the primary source and increases the power supplied to the plate. On the other hand, if the sampling period is less than the sing-around time, it finds the optimal vibration attenuation condition by maximizing wave absorption. Whether the sampling period exceeds the sing-around time or not was crucial for the one-dimensional case (see Figure 18), but does not seem to be so crucial in two dimensions. The convergence value and the corresponding vibration reduction gradually decrease as the sampling period increases. This is explained by the fact that most of the waves reflected by the controller do not reach the primary source of vibration directly, but through many reflections in the two-dimensional field. Thereby, the response of the control appears as the one between the two extreme cases. In this sense, the sampling period does not necessarily have to be within one sing-around time, but obviously shorter periods give better results.

6. CONCLUSIONS

To achieve non-application-specific active control, a controller called a ''maximum power abosorber'' was developed based on the proposed control strategy, where power absorbed by the controller is maximized within a sing-around time. This controller was applied to three kinds of experimental vibration problems, the first one a string, the second acoustic waves in a tube and the third a plate problem. The validity of the controller was studied and explored through these applications. It has been revealed that the proposed control strategy is applicable to a wide range of vibration problems. This result suggests that an optimal damper which extracts power maximally from a vibrating field within one sing-around time attenuates the vibration effectively. This is so for discrete frequency and broadband vibration fields.

ACKNOWLEDGMENTS

The author wishes to thank Professor J. E. Ffowcs Williams for supervising this work and Professor A. P. Dowling for useful discussions. He also gratefully acknowledges the financial support of Emmanuel College and ORS Awards Scheme during the course of this work.

REFERENCES

1. N. Hirami 1997 *Journal of Sound and Vibration* **200**, 243–259. Optimal energy absorption as an active noise and vibration control strategy.
2. J. E. Ffowcs Williams 1988 *Inter-Noise* **88**, 5–20. Active control of ''noisy'' systems.
3. W. Redman-White, P. A. Nelson and A. R. D. Curtis 1987 *Journal of Sound and Vibration* **112**, 187–191. Experiments on the active control of flexural wave power flow.

4. D. GUICKING, J. MELCHER and R. WIMMEL 1989 *Acustica* **69**, 39–52. Active impedance control in mechanical structures.
5. N. HIRAMI 1994 *British Patent Application No*. 9411154.9. Improvement in active control.
6. T. H. ROCKWELL and J. M. LAWTHER 1964 *Journal of Acoustical Society of America* **36**, 1507–1515. Theoretical and experimental results on active vibration dampers.